ASIAN JOURNAL OF PHARMACEUTICAL SCIENCES 10 (2015) 363–371

HOSTED BY

Available online at www.sciencedirect.com

ScienceDirect

journal homepage: www.elsevier.com/locate/ajps

Original Research Paper

Lipid-albumin nanoassemblies co-loaded with borneol and paclitaxel for intracellular drug delivery to C6 glioma cells with P-gp inhibition and its tumor targeting

Bo Tang [a], *Guihua Fang* [a], *Ying Gao* [a], *Yi Liu* [a], *Jinwen Liu* [a], *Meijuan Zou* [a], *Lihong Wang* [b], *Gang Cheng* [a,*]

[a] *School of Pharmacy, Shenyang Pharmaceutical University, 103 Wenhua Road, Shenyang 110016, China*
[b] *School of Pharmaceutical Engineering, Shenyang Pharmaceutical University, 103 Wenhua Road, Shenyang 110016, China*

ARTICLE INFO

Article history:
Received 5 April 2015
Received in revised form 23 April 2015
Accepted 27 April 2015
Available online 12 May 2015

Keywords:
Borneol
Paclitaxel
Lipid-albumin nanoassemblies
C6 glioma cells
P-gp inhibition

ABSTRACT

Successful chemotherapy with paclitaxel (PTX) is impeded by multidrug resistance (MDR) in tumor cells. In this study, lipid-albumin nanoassemblies co-loaded with borneol and paclitaxel (BOR/PTX LANs) were prepared to circumvent MDR in C6 glioma cells. The physiochemical properties including particle size, encapsulation efficiency and morphology were evaluated *in vitro*. Quantitative and qualitative investigations of cellular uptake were carried out in C6 glioma cells. The cytotoxicity of the BOR/PTX LANs was determined by MTT assay. After that, the tumor targeting was also evaluated in C6 glioma bearing mice by *in vivo* imaging analysis. BOR/PTX LANs have a higher entrapment efficiency (90.4 ± 1.2%), small particle size (107.5 ± 3.2 nm), narrow distribution (P.I. = 0.171 ± 0.02). The cellular uptake of PTX was significantly increased by BOR/PTX LANs compared with paclitaxel loaded lipid-albumin nanoassemblies (PTX LANs) in quantitative research. The result was further confirmed by confocal laser scanning microscopy qualitatively. The cellular uptake was energy-, time- and concentration-dependent, and clathrin- and endosome/lysosome-associated pathways were involved. The BOR/PTX LANs displayed a higher cytotoxicity agaist C6 glioma cells in comparion with PTX LANs and Taxol. Moreover, the encapsulation of BOR in LANs obviously increased the accumulation of the drug in tumor tissues, demonstrating the tumor targeted ability of BOR/PTX LANs. These results indicated that BOR/PTX LANs could overcome MDR by combination of drug delivery systems and P-gp inhibition, and shown the potential for treatment of gliomas.

* *Corresponding author*. School of Pharmacy, Shenyang Pharmaceutical University, China.
E-mail address: chenggang63@hotmail.com, chenggangsypha@163.com (G. Cheng).
Peer review under responsibility of Shenyang Pharmaceutical University.
http://dx.doi.org/10.1016/j.ajps.2015.04.004

1. Introduction

Gliomas are the most common primary brain tumors. It accounts for about 80% of all brain tumors, with an incidence rate of approximately 7 per 100,000 worldwide. Patients with gliomas may have several neurological symptoms such as headaches, seizures, memory loss, vomiting, visual changes and so on [1–3]. Gliomas are resistant to many therapy methods, including chemotherapy, radiation and other adjuvant therapies. The failure of chemotherapy in gliomas is often due to the development of multidrug resistance (MDR) by tumor cells. Over the past years, various mechanisms of MDR have been proposed, including the overexpression of MDR pumps like P-glycoprotein (P-gp) [4], reduced in topoisomerase activity [5], modifications in glutathione metabolism [6] or altered expression of apoptosis-associated protein Bcl-2 [7] and tumor suppressor protein p53 [8]. One of the major cause is due to the overexpression of membrane-bound proteins such as P-gp. Many P-gp substrates such as doxorubicin and paclitaxel (PTX) were expelled out of the tumor cells, resulting in the reduction of accumulation of drugs in the tumor cells, thereby causing the treatment failure [9]. On the other hand, treatment with high doses or combination chemotherapy is insufficient to inhibit the function of P-gp. In addition, these treatments are often related to toxic side effects in patients, because most antitumor drugs do not have specificity towards the tumor cells [10]. Several therapeutic strategies have been explored for overcoming MDR.

Nano-drug delivery systems, such as liposomes, lipid nanoparticles, polymeric micelles and microemulsions have gained much attention to overcome MDR [11]. Firstly, they could improve the solubility of drugs. Secondly, the nanocarriers could enter into the glioma cells by endocytosis, which was able to circumvent MDR of the tumor cells [12]. In addition, the nanocarriers were expected to act as the intracellular drug reservoirs after entering the tumor cells, which could protect antitumor drugs from degradation and increase the drug efficacy [13]. However, most of the free drugs were still expelled by the P-gp in tumor cells [14,15].

P-gp inhibitors have been extensively investigated for inhibiting P-gp efflux pump [16]. Different generations of pharmacological P-gp inhibitors have been studied in last decades, but most of the drug trials were disappointing as the inhibitors exhibited high systemic toxicity [17]. Other factors such as the limited solubility of P-gp inhibitors in aqueous solution have also contributed to the failure of P-gp inhibitors in overcoming MDR. To date, co-encapsulation of P-gp substrates and P-gp inhibitors in nanocarriers was a promising alternative for enhancing the anti-tumor drugs uptake in the tumor cells. Verapamil, a first generation p-gp inhibitor, has been reported to be able to reverse completely the resistance caused by P-gp *in vitro*[18]. It was reported that the intracellular accumulation of PTX was significantly increased, and the PTX was more effective in inhibiting the growth of the tumor cells when it was co-encapsulated with verapamil in polymer micelles [19,20]. In recent studies, the third-generation P-gp modulator, tariquidar, was co-encapsulated with paclitaxel in long circulating liposomes. The co-loaded liposomes resulted in about 100-fold lower IC_{50} than paclitaxel liposomes. Therefore, it is effective to overcome MDR of the tumor cells by co-encapsulation of the P-gp inhibitors and the anti-tumor drugs using a nano-drug delivery system [21].

Borneol (BOR), a simple bicyclic monoterpene, is widely used in traditional Chinese medicine, such as the "Xingnaojing" injection. Some studies have demonstrated that borneol is able to loosen intercellular tight junctions [22] and inhibit the action of P-gp on the cell membrane [23]. We speculate that co-encapsulation of BOR and PTX could increase the uptake of PTX by the brain glioma cells.

In our previous work, we have prepared PTX-loaded lipid-protein nanoparticles, which exhibited high drug entrapment efficiency, small particle size and good biocompatibility [24]. In the current research, the BOR and PTX were co-encapsulated in the lipid-albumin nanoassemblies to achieve higher cellular uptake and stronger anti-tumor efficacy in C6 glioma cells by inhibiting P-gp. Additionally, the tumor-targeted efficacy was also increased in glioma-bearing mice.

2. Materials and methods

2.1. *Materials*

Paclitaxel (PTX) was obtained from Tianfeng Bioengineering Technology Co., Ltd. (Liaoning, China). Borneol (BOR) was obtained from Yunnan Linyuan spicery Co., Ltd. (Yunnan, China). Egg yolk lecithin PL 100M was purchased from the Q.P. Corporation (Tokyo, Japan), Cremophor EL was kindly gifted by the BASF Corporation (Ludwigshafen, Germany), 3-(4, 5-Dimethylthiazol-2-yl)-2, 5-diphenyl- tetrazoliumbromide (MTT), Bovine serum albumin (BSA) and Rhodamine 6G were obtained from Sigma–Aldrich (St. Louis, MO, USA). Penicillin–streptomycin, DMEM, fetal bovine serum (FBS) and 0.25% (w/v) trypsin–0.03% (w/v) EDTA solution were obtained from Gibco BRL (Gaithersberg, MD, USA). 4, 6- diamidino- 2 -phenylindole (DAPI), BCA kit and Triton X-100 were purchased from Beyotime Biotechnology Co., Ltd. (Nantong, China). 4% paraformaldehyde was obtained from Solarbio Technology Co., Ltd. (Beijing, China). 1, 1′-Dioctadecyl-3, 3, 3′, 3′- tetramethylindotricarbocyanine Iodide (DIR) was purchased from Biotium (Hayward, CA). All other chemicals and solvents were of analytical or chromatographic grade.

Taxol injection was prepared according to the clinical formulation. PTX (0.012 g) was dissolved in anhydrous ethanol (1 ml) and cremophor EL (1 ml) under magnetic stirring. Taxol injection was diluted with saline before test [25].

The C6 giloma cells were gifted by Prof. Jingyu Yang (Department of Pharmacology, Shenyang Pharmaceutical University, Shenyang, China). The cells were cultured in DMEM medium, supplemented with 10% FBS, 100 IU/ml penicillin and 100 μg/ml streptomycin sulfate. All the cells were grown in incubators maintained at 37 °C with 5% CO_2 under fully humidified conditions. All experiments were performed on cells during the logarithmic phase of growth.

Male Kunming mice (18–22 g) were obtained from the Experimental Animal Center (Shenyang Pharmaceutical University, China). All the animal experiments were approved by Shengyang Pharmaceutical University Ethics Committee and according to the Guidelines for the Use of Laboratory Animals.

2.2. Preparation of BOR/PTX LANs

The BOR/PTX LANs were prepared by a desolvation-ultrasonication technique as described in our previous work [24]. In brief, 5 ml of BSA aqueous solution was prepared at a concentration of 40 mg/ml, BOR (0.01 g), PTX (0.01 g) and PL 100M (0.10 g) were dissolved in 0.3 ml anhydrous ethanol, and then the ethanol solution were added dropwise to the BSA solution with stirring at room temperature. The resulting mixture was sonicated by a probe ultrasonication (JY92-II, Ningbo, China). Then, the anhydrous ethanol was removed by rotary evaporation. Then, the samples were centrifuged and passed through a 0.22 μm filter membrane to obtain BOR/PTX LANs.

The preparation method for borneol and rhodamine 6G co-loaded LANs (BOR/RDM LANs) was the same as that for BOR/PTX LANs, except that PTX was replaced with rhodamine 6G. Rhodamine 6G loaded LANs (RDM LANs) were prepared using the same procedure, except for without addition of BOR.

The preparation method for borneol and DIR co-loaded LANs (BOR/DIR LANs) was the same as that for BOR/PTX LANs, except that PTX was replaced with DIR. DIR loaded LANs (DIR LANs) were prepared using the same procedure, except for without addition of BOR.

2.3. Determination of entrapment efficiency

The entrapment efficiency of BOR/PTX LANs was determined as described in our previous study [24]. The solubility of PTX in BOR/PTX LANs (>1.6 mg/ml) was far higher than that of free PTX in water (<1 μg/ml). Therefore, the amount of free PTX in BOR/PTX LANs could be neglected. In order to determine the weight of drug in BOR/PTX LANs, acetonitrile was used to precipitate BSA, and release PTX from the BOR/PTX LANs. After centrifugation at 12,000 rpm for 10 min, 20 μl of the supernatant was injected into an HPLC system. The drug encapsulation efficiency (EE) was calculated as follows:

$$EE(\%) = \frac{W_{\text{total drug}}}{W_{\text{feeding drug}}} \times 100$$

Where, $W_{\text{total drug}}$ represents the weight of drug in BOR/PTX LANs, $W_{\text{feeding drug}}$ represents the weight of feeding drug.

2.4. Characterization of BOR/PTX LANs

The size distribution, polydispersity index (P.I.) of the BOR/PTX LANs were evaluated by dynamic light scattering (DLS) (PSS NICOMP 380, USA). The morphology was observed using transmission electron microscopy (TEM) (JEOL, Tokyo, Japan).

2.5. Cellular uptake

2.5.1. Cellular uptake of PTX

Cellular uptake of PTX was determined in the presence or absence of known various concentrations of BOR ranging from 0.001 to 10.0 μg/ml in C6 glioma cells. Cyclosporine A (CsA) was used as positive control, and the inhibition concentration was set at 20.0 μg/ml throughout the studies. C6 cells (2×10^5 per 1 ml/well) were seeded in 24-well plates and incubated for 24 h. After they reached 80% confluence, Taxol solution (50 μg/ml) with various concentrations of BOR were incubated for 2 h at 37 °C. After 2 h incubation, the cells were washed with ice-cold PBS for 3 times, the cells were lysed with 0.3 ml of 1% Triton X-100. The concentration of PTX in cell lysate was determined using HPLC method described above. The cell protein content was determined by the BCA protein assay kit. Cellular uptake efficiency (%) was calculated as the following equation.

$$\text{Cellular uptake efficiency}(\%) = (C_s/P_s)/(C_c/P_c) \times 100$$

Where C_s represents the PTX concentration of sample, P_s represents the protein content of sample, C_c represents the PTX concentration of control, and P_c represents the protein content of control.

2.5.2. The effect of incubation time on cellular uptake

The time-dependent internalization of PTX with or without BOR (1.0 μg/ml) was evaluated in C6 glioma cells at predetermined time intervals (0.5, 1.0 and 2.0 h), cellular uptake was conducted as described above.

2.5.3. Cellular uptake of BOR/PTX LANs

Cellular uptake of PTX from Taxol solution, PTX LANs and BOR/PTX LANs with BOR (or CsA) or without BOR (or CsA) were evaluated in C6 glioma cells after 2.0 h incubation. The cellular uptake experiment was conducted as described above.

2.5.4. Confocal microscopy studies

For the qualitative study, C6 glioma cells (2×10^4 per 1 ml/well) were seeded in 24-well plates and incubated for 24 h. The cells were washed and incubated with Rhodamine 6G solution (RDM solution), RDM LANs and BOR/DIR LANs at 37 °C for 2 h. Then the cells were washed with ice-cold PBS for 3 times, and fixed with 4% paraformaldehyde for 20 min. The nuclei were counterstained by DAPI. The coverslips were mounted on microscope slides and the intracellular accumulation was visualized under confocal laser scanning microscope (Leica, Germany). The time- and concentration-dependent cellular uptake were evaluated.

2.5.5. Uptake mechanism

C6 glioma cells (2×10^5 per 1 ml/well) were seeded in 24-well plates and incubated for 24 h. After checking the confluency and morphology, various inhibitors of PBS (control), chlorpromazine (10 μg/ml), sodium azide (3 μg/ml), colchicines (8 μg/ml), indomethacin (6 μg/ml), quercetin (6 μg/ml), amonium chloride (10 mM) were added and incubated for 1 h. Then the medium was withdrawn from the wells and the PTX LANs (50 μg/ml) and BOR/PTX LANs (50 μg/ml) were added. After 2 h incubation, the cells were processed and cellular uptake efficiency (%) was calculated as described above. In order to investigate the effect of temperature on the cellular uptake, the cells were also incubated under both 37 °C and 4 °C.

2.6. In vitro cytotoxicity

The cell viability was measured using the methylthiazoletetrazolium (MTT) method. In order to determine the toxicity of

different formulations, C6 glioma cells were seeded in 96-well plates at a density of 5.0×10^3 cells/well. After 24 h incubation, the cells were treated with 200 μl medium containing Taxol solution, PTX LANs and BOR/PTX LANs at serial concentrations, respectively. After 72 h incubation, a total of 20 μl MTT (5 mg/ml) and 180 μl fresh medium were supplied to each well followed by incubation for another 4 h, and then the formazan crystals were dissolved in 200 μl DMSO. The absorbance at 492 nm of each well was measured in a microplate reader (Model 500, USA). Cell viability was determined and IC_{50} values were calculated using nonlinear regression analysis.

2.7. *In vivo image*

In vivo real-time fluorescence imaging analysis was used to evaluate the effect of the biodistribution of nanoparticles. The tumor model was established by injecting subcutaneously of 3×10^7 C6 cells in the right flanks of the mice. After 10 days, the mice were randomly divided into three groups ($n = 3$) and were i.v. administrated via tail vein injection with DIR solution, DIR LANs and BOR/DIR LANs at a dose of 5 mg/kg. Then, the mice were scanned at 1, 2, 4, 8, 12 and 24 h using an Fx Pro multimodal imaging system (Bruker Corp., USA).

In order to further observe the distribution in tumor masses and the major organs, the tumor-bearing mice were sacrificed at 24 h after heart perfusion with saline and 4% paraformaldehyde, followed by immediate removal of the brain, heart, liver, spleen, lung, kidney and tumor masses. The fluorescence signal intensities in different tissues were photographed.

2.8. *Statistical analysis*

Analysis of statistical significance was performed with the SPSS statistics software16.0. The data are presented as the mean ± SD. Student's t-test was used to analyze the differences. The differences were considered significant at $P < 0.05$.

3. Results and discussion

3.1. *Characterization of BOR/PTX LANs*

Particle size is a key factor determining the distribution of nano-drug delivery system. It not only affects the nanoparticles entering into tumor cells but also affects the drug accumulation in tumor site. The particle size was determined by DLS analysis (Fig. 1). The average size of the PTX LANs and BOR/PTX LANs were 113.2 ± 4.5 nm, 107.5 ± 3.2 nm, respectively. Therefore, most of the the PTX LANs or BOR/PTX LANs have the potential to accumulate in tumor tissue by EPR effect [26]. Both PTX LANs and BOR/PTX LANs have high entrapment efficiency of 92.5 ± 1.8%, 90.4 ± 1.2%, respectively. The morphology of the LANs was also shown in Fig. 1, they were spherical in shape, an aqueous core surrounded by a multilayer structure (lipid bilayers separated by a BSA-water interlayer). The BOR/PTX-BSA conjugate located in the interlayer of the LANs. Both BOR and PTX are hydrophobic and bind to albumin with high affinity [27,28], and thus BOR/PTX can tightly bound to BSA to form a BOR/PTX-BSA conjugate via hydrophobic interactions. Then, the interactions between the BOR/PTX-BSA conjugate and phosphatidylcholine molecule contribute to the formation of the BOR/PTX LANs.

3.2. *Cellular uptake*

3.2.1. *Cellular accumulation of PTX*

In order to investigate the potential effect of BOR on P-gp mediated efflux, the cellular uptake of PTX was studied in C6 glioma cells in comparison with that of CsA, a typical P-gp inhibitor. As shown in Fig. 2, compared with Taxol, the cellular uptake of Taxol (50 μg/ml PTX) with CsA (20 μg/ml) increased markedly than that of Taxol without CsA. It is suggested that BOR have an effect on inhibiting P-gp efflux pumps. In addition, the accumulation of PTX increased gradually with increasing concentrations of BOR (0.001–1.0 μg/ml), and then reached a plateau over a wide range of concentrations of BOR (1.0–10.0 μg/ml). The result suggested that the effect of BOR on inhibiting P-gp efflux pumps exhibits concentration dependence and saturation properties. Furthermore, the cellular uptake of PTX was greater than or equal to the standard P-gp inhibitor CsA over a wide range of concentrations of BOR (1.0–10.0 μg/ml). Moreover, the time dependence of PTX accumulation was evaluated over 2 h with or without BOR (Fig. 3). Taxol with BOR (1.0 μg/ml) shown an obvious increase in PTX accumulation compared to Taxol alone at the time point of 1 h and 2 h.

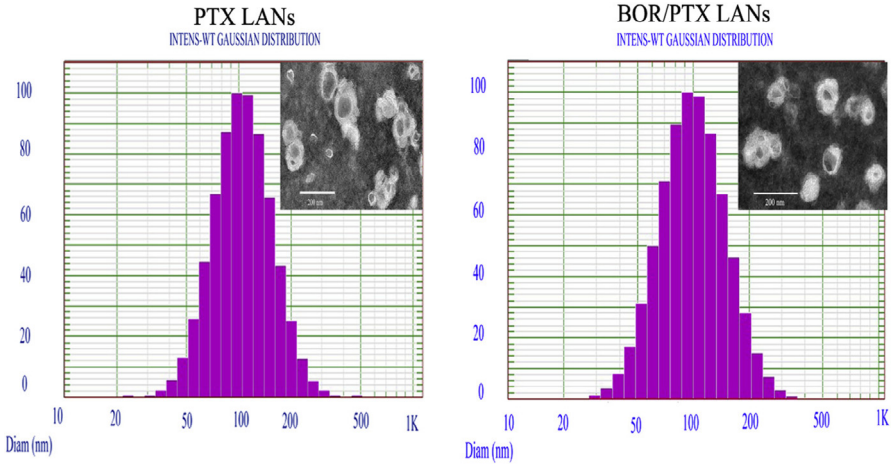

Fig. 1 – Size distribution and TEM image of PTX LANs, BOR/PTX LANs. (scale bar 200 nm in TEM image).

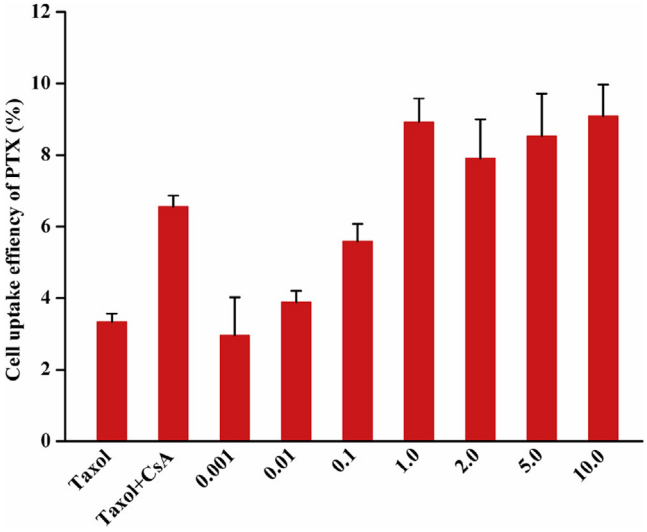

Fig. 2 – Effect of BOR on cellular uptake of PTX at 37 °C for 2 h. Taxol: 50 μg/ml. CsA: 20 μg/ml. The concentration range of BOR was 0.001–10.0 μg/ml (n = 3).

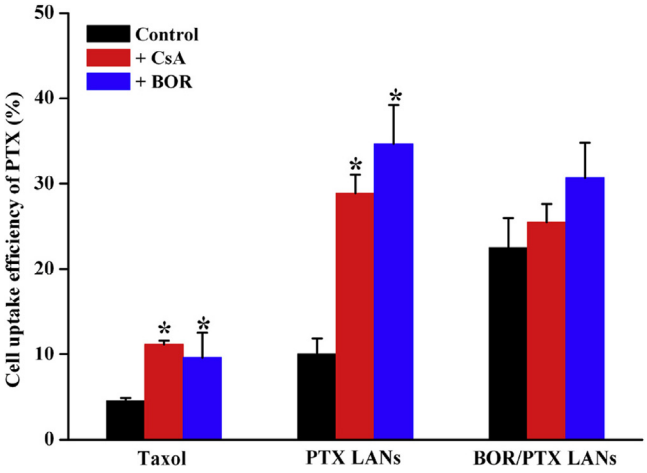

Fig. 4 – Effect of BOR on cellular uptake of PTX LANs and BOR/PTX LANs at 37 °C for 2 h. Taxol, PTX LANs and BOR/PTX LANs: 50 μg/ml. CsA: 20 μg/ml. BOR: 1.0 μg/ml *P < 0.05, compared with Control. (n = 3).

The cellular uptake of LANs was also evaluated in C6 cells after 2 h incubation (Fig. 4). BOR/PTX LANs showed more uptake in comparison with the other formulations. The celluar uptake of BOR/PTX LANs and PTX LANs showed 4.96-fold and 2.20-fold increase compared with Taxol, respectivly. To confirm the p-gp inhibition by BOR/PTX LANs, additional free CsA and BOR was added in the incubation of C6 cells. The additional free CsA and BOR along with PTX LANs significantly enhanced PTX uptake to 2.89-fold and 3.46-fold, respectively. However, the addition of free CsA or BOR along with BOR/PTX LANs hardly increased the PTX uptake. This indicated that BOR/PTX LANs had sufficient ability to inhibit P-gp efflux of PTX without additional CsA or BOR.

3.2.2. *Confocal scanning microscopy*

The confocal scanning microscopy was employed to visualize the internalization and distribution of the LANs in C6 cells (Fig. 5). Both RDM LANs and BOR/RDM LANs showed higher intensity of fluorescence than RDM solution at different concentration (or different time). The results demonstrated that the LANs could significantly increase the cellular uptake. It could also be observed that the BOR/RDM LANs had the strongest intensity of fluorescence at different concentration (or different time). This can be ascribed to the BOR, as a P-gp inhibitor, which could reduce intracellular RDM (P-gp substrates) efflux to improve the cellular uptake. Moreover, at the same time, the cellular uptake of RDM LANs and BOR/RDM LANs could be obviously improved with increasing concentration, suggesting concentration-dependent properties in the uptake of LANs. Additionally, at the same concentration, the cellular uptake of PTX LANs and BOR/PTX LANs could also be significantly enhanced with elevating the incubation time, implying time-dependent properties in the cellular uptake of the LANs.

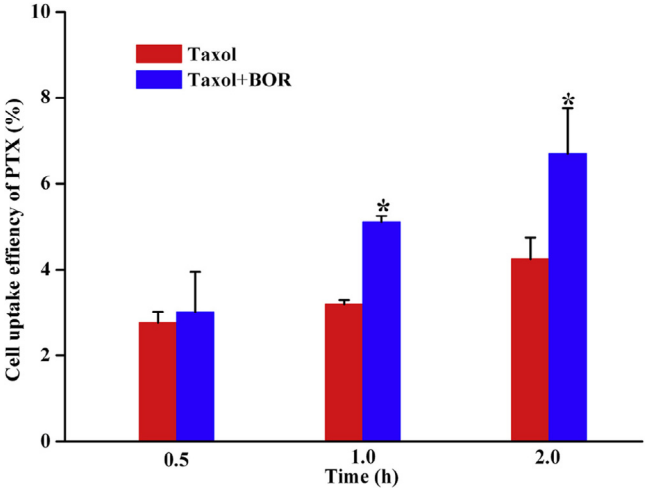

Fig. 3 – The time-dependent cellular uptake of PTX. Taxol: 50 μg/ml. BOR: 1.0 μg/ml *P < 0.05, compared with Taxol. (n = 3).

3.2.3. *Uptake mechanism*

In order to clarify the internalization mechanism of the LANs by C6 cells, the effects of various endocytosis inhibitors on cellular uptake were investigated quantitatively. Chlorpromazine, colchicine, indomethacine, quercetin and ammonium chloride were used to block clathrin-associated, macropinocytosis-associated, caveolin-associated, clathrin- and caveolin-independent and lysosome-associated endocytosis pathway respectively. Sodium azide and 4 °C were employed to evaluate the effect of energy on the cellular uptake. As shown in Fig. 6, the cellular uptake was hindered significantly in the presence of chlorpromazine, suggesting that clathrin was involved in the internalization of LANs. Ammonium chloride, a lysosomotropic agent that inhibited the acidification of endosome/lysosome, which decreased significantly the uptake of LANs. This result indicated the endosome/lysosome pathway was involved. Both 4 °C and sodium amide exhibited strongest inhibition of cellular uptake, showing energy-dependent properties in the uptake of LANs. On the contrary, colchicine, indomethacine and quercetin, had no impact on the uptake,

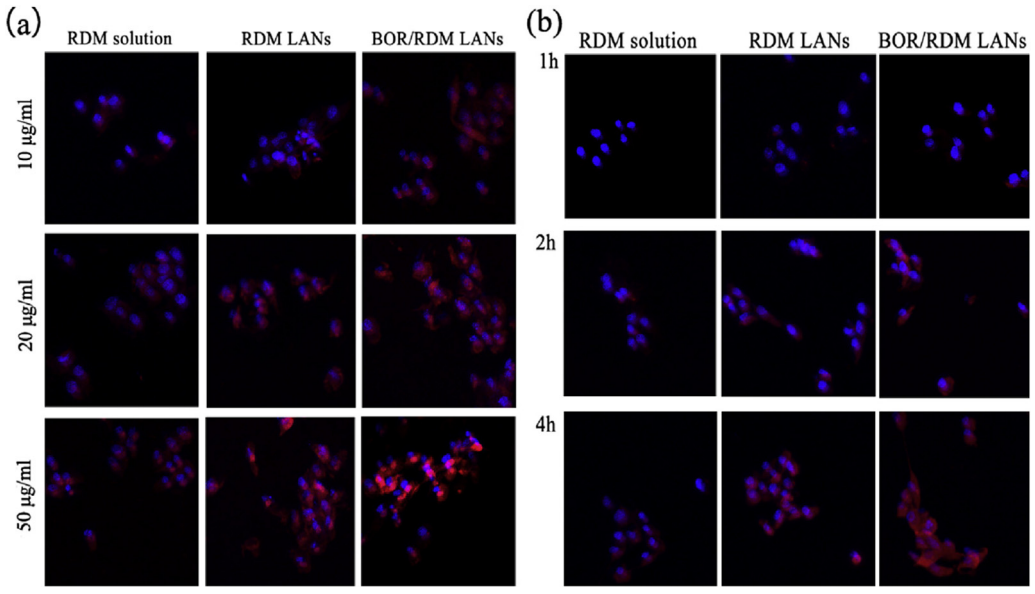

Fig. 5 – The confocal microscopy images showing cellular uptake of Rhodamine 6G (RDM) from different formulations: The concentration-dependent uptake after 2 h incubation (a) and time-dependent uptake at the RDM concentration of 10 μg/ml (b). Original magnification: 10 × 20.

suggesting that the endocytosis of PTX-LANs and BOR/PTX LANs was not via macropinocytosis, caveolin-associated, clathrin- and caveolin-independent endocytosis. Accordingly, the cellular uptake of PTX-LANs and BOR/PTX LANs by C6 cells was mainly mediated by clathrin and endosome/lysosome-associated pathway. Moreover, both PTX LANs and BOR/PTX LANs had similar uptake mechanism. It was reported that the transport pathway of nanoparticles in cells depends on structure and physicochemical characteristics of nanoparticles (size, shape, charge, surface properties, etc.), as well as cell types [29].

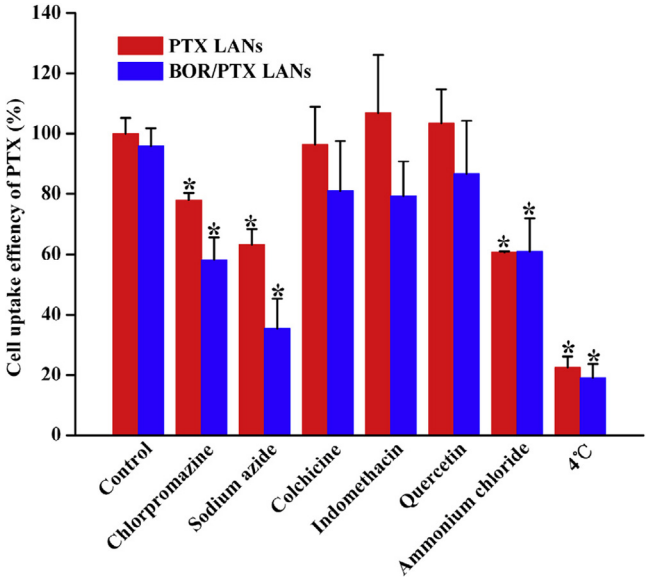

Fig. 6 – Effects of inhibitors and temperature on cellular uptake of PTX LANs and BOR/PTX LANs at equal PTX concentration of 50 μg/ml after 2 h incubation with C6 glioma cells. *P < 0.05, compared with Control. (n = 3).

The result might be related to the similarity in structure and physicochemical characteristics between PTX LANs and BOR/PTX LANs.

3.3. *Cytotoxicity*

In order to investigate whether the increased intracellular PTX accumulation by BOR/PTX LANs could increase its cytotoxicitys in tumor cells. The cytotoxicity of PTX from different formulations was tested against C6 glioma cells, and cell viability was determined by the MTT assay after 72 h incubation. The comparison of IC_{50} values of Taxol, PTX LANs and BOR/PTX LANs was shown in Table 1. Taxol and PTX LANs showed higher IC_{50} values of 1.54 μg/ml, 1.66 μg/ml in comparision with that of BOR/PTX LANs (0.96 μg/ml). The results indicated that the cytotoxicity of Taxol and PTX LANs was almost the same from the IC_{50} values. The cytotoxity of Taxol was attributed partially to the Cremophor EL [30,31], whereas, the cytotoxicity of the PTX LANs was only attributed to PTX. In particular, the BOR/PTX LANs showed the lowest IC_{50} values, suggesting that the BOR/PTX LANs did increased cytotoxicity against C6 glioma cells. Two major reasons can be account for enhanced cytotoxicity of BOR/PTX LANs in C6 cells. First, an increased extent of drug uptake by endocytosis of nanoparticles, which helps to partially bypass P-gp; second, a decreased efflux rate of drug through inhibition of P-gp function by BOR.

Table 1 – IC_{50} values of the different PTX loaded LANs formulations compared to Taxol. (n = 3).

Formulations	Taxol	PTX LANs	BOR/PTX LANs
IC_{50} (μg/mL)	1.54 ± 0.09	1.66 ± 0.12	0.96 ± 0.08*

*P < 0.05, compared with Taxol or PTX LANs.

Paclitaxel is a well-known anticancer drug, which has been used in the treatment of wide range of cancers but its entry into cancer cell is restricted by P-gp [32,33]. It was reported that co-encapsulation of P-gp inhibitor and anticancer drug in nanoparticles was an effective method to overcome P-gp efflux in cancer chemotherapy, which can significantly improve the cellular uptake of anticancer drugs [34–36]. In our study, we encapsulated BOR in LANs to inhibit the P-gp efflux of PTX. *In vitro* uptake experiments demonstrated that co-encapsulation of BOR and PTX in LANs significantly increased the drug uptake in comparison with that of Taxol and PTX LANs. Thus, BOR/PTX LANs have the ability to inhibit P-gp efflux pumps, resulting in a reduction of drug efflux and increasing the intracellular accumulation of PTX. On basis of above mentioned results, three reasons contributed to the enhancement of cellular uptake. Firstly, after BOR/PTX LANs enter into cells, the intracellular released BOR from BOR/PTX LANs could inhibit P-gp efflux, and further increase the cellular accumulation of PTX. Secondly, endocytosis of BOR/PTX LANs was ATP-consuming process, which could reduce the activity of P-gp. Finally, the composition of the LANs was similar to the cell membrane consisting of lipids and proteins, which probably have higher affinity to the cell membrane of tumor cells, and thus increasing the LANs entry the tumor cells by endocytosis. In a word, the more drugs were accumulated, the higher cytotoxicity against tumor cells could be obtained.

3.4. *In vivo image*

To evaluate the targeting effect of BOR/PTX LANs, C6 xenograft bearing mice were used for *in vivo* imaging analysis. DIR-labeled LANs were given intravenously into C6 tumor bearing mice through the tail vein, and the DIR solution was used as negative control. As shown in Fig. 7a, the fluorescence signal was viewed in the tumor-bearing mice as early as 1 h after injection. The maximum fluorescence signal was observed at 2 h post-injection with gradually decrease after 24 h post-injection. The fluorescence signal of LANs in the brain was higher compared with DIR solution after i.v. administration. BOR/DIR LANs has the strongest fluorescence signal until 24 h post-injection. These results suggested that LANs could passively distribute and accumulate in C6 xenografts by EPR effect. Moreover, co-encapsulation with BOR could inhibit the P-gp mediated efflux and further increase the accumulation of DIR in tumor site.

In order to investigate the tissue distribution of the LANs, the *ex vivo* fluorescent images of the tissues were captured after

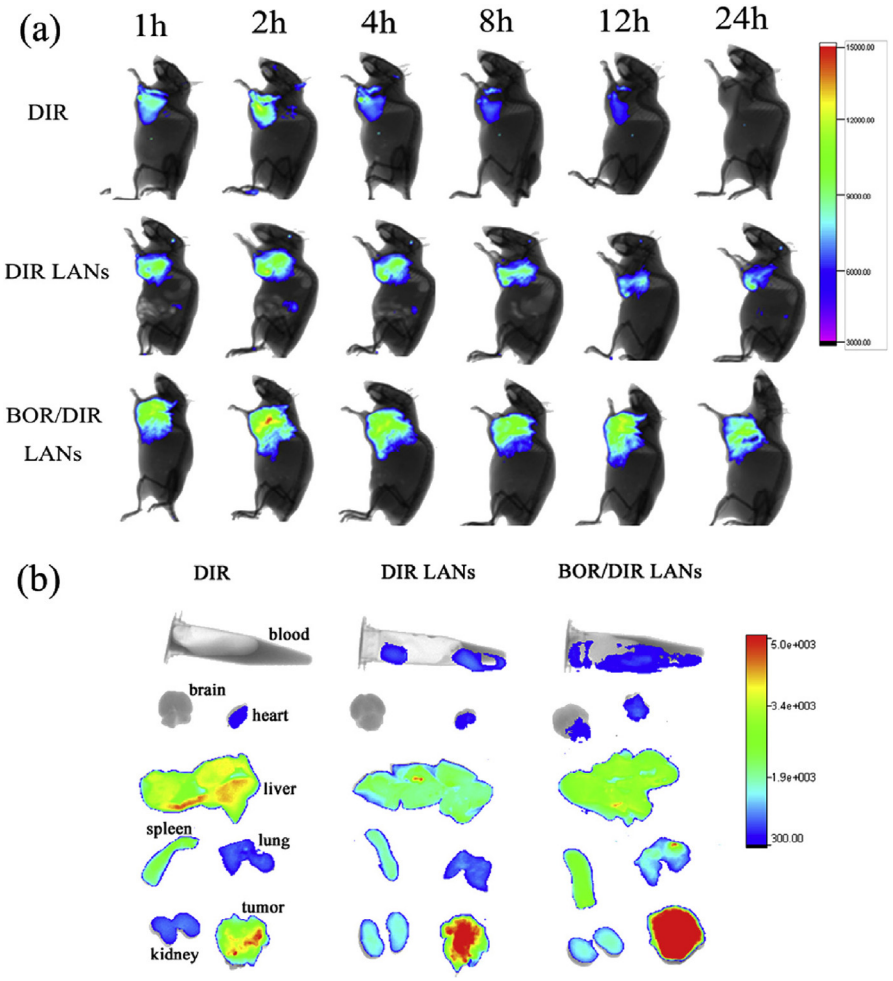

Fig. 7 – *In vivo* and *ex vivo* imaging. Fluorescent imaging of glioma bearing mice after i.v. administration with DIR solution, DIR LANs and BOR/DIR LANs at dose of 5 mg/kg (a); *ex vivo* imaging at 24 h (b).

24 h. As shown in Fig. 7b, the distribution of LANs in liver was lower than that of DIR solution, indicating that LANs could reduce toxicity in liver. Importantly, the distribution of BOR/DIR LANs in tumor masses was higher than that of DIR LANs, suggesting that co-encapsulation with BOR in LANs could increase the distribution in tumors tissue and reduce its in liver.

Therefore, the BOR/PTX LANs could be a potential nano-drug delivery system to enhance the anti-glioma effect. Further studies in tumor models are needed to determine the *in vivo* efficacy of BOR/PTX LANs.

4. Conclusion

Lipid-albumin nanoassemblies co-loaded with BOR and PTX were prepared and characterized. Compared with PTX LANs, BOR/PTX LANs significantly enhanced cytotoxicity in C6 glioma cells. The cellular uptake of LANs was energy-, time- and concentration-dependent, and clathrin- and endosome/lysosome-associated pathways were involved. Furthermore, *in vivo* image indicated that co-encapsulation of BOR in LANs could obviously increase the accumulation of drug in tumor tissues in comparison with the LANs without BOR. Therefore, BOR/PTX LANs might be a promising drug delivery system for improving the efficacy of chemotherapy by the combination of drug delivery and P-gp inhibition.

Acknowledgements

The authors thank Prof. Jingyu Yang of Shenyang Pharmaceutical University for kindly providing the cells, and Associate Prof. Mingyu Xia and Prof. Takashi Ikejima of Shenyang Pharmaceutical University for their helpful advice and assistance in the cell culture experiments.

REFERENCES

[1] Ferguson SD. . Malignant gliomas: diagnosis and treatment. Dis Mon 2011;57:558–569.
[2] Chandana SR, Movva S, Arora M, et al. Primary brain tumors in adults. Am Fam Physician 2008;77:1423–1430.
[3] Wen PY, Kesari S. . Malignant gliomas in adults. N Engl J Med 2008;359:492–507.
[4] Krishnamachary N, Center MS. . The MRP gene associated with a non-P-glycoprotein multidrug resistance encodes a 190-kDa membrane bound glycoprotein. Cancer Res 1993;53:3658–3661.
[5] Deffie AM, Batra JK, Goldenberg GJ. . Direct correlation between DNA topoisomerase II activity and cytotoxicity in adriamycin-sensitive and-resistant P388 leukemia cell lines. Cancer Res 1989;49:58–62.
[6] Zhang L, Schaner ME, Giacomini KM. . Functional characterization of an organic cation transporter (hOCT1) in a transiently transfected human cell line (HeLa). J Pharmacol Exp Ther 1998;286:354–361.
[7] Kirkin V, Joos S, Zörnig M. . The role of Bcl-2 family members in tumorigenesis. Biochimica Biophysica Acta (BBA)-Mol Cell Res 2004;1644:229–249.
[8] Viktorsson K, De Petris L, Lewensohn R. . The role of p53 in treatment responses of lung cancer. Biochem Biophys Res Commun 2005;331:868–880.
[9] Gottesman MM, Fojo T, Bates SE. . Multidrug resistance in cancer: role of ATP–dependent transporters. Nat Rev Cancer 2002;2:48–58.
[10] Yagüe E, Arance A, Kubitza L, et al. Ability to acquire drug resistance arises early during the tumorigenesis process. Cancer Res 2007;67:1130–1137.
[11] Bansal T, Akhtar N, Jaggi M, et al. Novel formulation approaches for optimising delivery of anticancer drugs based on P-glycoprotein modulation. Drug Discov Today 2009;14:1067–1074.
[12] Jabr-Milane LS, van Vlerken LE, Yadav S, et al. Multi-functional nanocarriers to overcome tumor drug resistance. Cancer Treat Rev 2008;34:592–602.
[13] Liang X-J, Chen C, Zhao Y, et al. Circumventing tumor resistance to chemotherapy by nanotechnology. Multi-drug resistance in cancer. Springer; 2010. p. 467–488.
[14] Wong HL, Bendayan R, Rauth AM, et al. A mechanistic study of enhanced doxorubicin uptake and retention in multidrug resistant breast cancer cells using a polymer-lipid hybrid nanoparticle system. J Pharmacol Exp Ther 2006;317:1372–1381.
[15] Chavanpatil MD, Patil Y, Panyam J. . Susceptibility of nanoparticle-encapsulated paclitaxel to P-glycoprotein-mediated drug efflux. Int J Pharm 2006;320:150–156.
[16] Palakurthi S, Yellepeddi VK, Vangara KK. . Recent trends in cancer drug resistance reversal strategies using nanoparticles. Expert Opin Drug Deliv 2012;9:287–301.
[17] Lee CH. . Reversing agents for ATP-binding cassette drug transporters. Multi-drug resistance in cancer. Springer; 2010. p. 325–340.
[18] Huang M, Liu G. . The study of innate drug resistance of human hepatocellular carcinoma Bel 7402 cell line. Cancer Lett 1998;135:97–105.
[19] Choi J-S, Li X. . The effect of verapamil on the pharmacokinetics of paclitaxel in rats. Eur J Pharm Sci 2005;24:95–100.
[20] Wang F, Zhang D, Zhang Q, et al. Synergistic effect of folate-mediated targeting and verapamil-mediated P-gp inhibition with paclitaxel-polymer micelles to overcome multi-drug resistance. Biomaterials 2011;32:9444–9456.
[21] Montesinos RN, Béduneau A, Pellequer Y, et al. Delivery of P-glycoprotein substrates using chemosensitizers and nanotechnology for selective and efficient therapeutic outcomes. J Control Release 2012;161:50–61.
[22] Chen ZZ, Lu Y, Du SY, et al. Influence of borneol and muscone on geniposide transport through MDCK and MDCK-MDR1 cells as blood-brain barrier in vitro model. Int J Pharm 2013;456:73–79.
[23] He H, Shen Q, Li J. . Effects of borneol on the intestinal transport and absorption of two P-glycoprotein substrates in rats. Arch Pharm Res 2011;34:1161–1170.
[24] Tang B, Fang G, Gao Y, et al. Liprosomes loading paclitaxel for brain-targeting delivery by intravenous administration: in vitro characterization and in vivo evaluation. Int J Pharm 2014;475:416–427.
[25] Liu Z, Chen K, Davis C, et al. Drug delivery with carbon nanotubes for in vivo cancer treatment. Cancer Res 2008;68:6652–6660.
[26] Davis ME, Shin DM. . Nanoparticle therapeutics: an emerging treatment modality for cancer. Nat Rev Drug Discov 2008;7:771–782.
[27] Hu L, Chen D-Y. . Application of headspace solid phase microextraction for study of noncovalent interaction of

borneol with human serum albumin. Acta Pharmacol Sin 2009;30:1573–1576.
[28] Paal K, Müller J, Hegedûs L. . High affinity binding of paclitaxel to human serum albumin. Eur J Biochem 2001;268:2187–2191.
[29] Chavanpatil MD, Khdair A, Panyam J. . Nanoparticles for cellular drug delivery: mechanisms and factors influencing delivery. J Nanosci Nanotechnol 2006;6:2651–2663.
[30] Liebmann J, Cook JA, Lipschultz C, et al. The influence of Cremophor EL on the cell cycle effects of paclitaxel (Taxol®) in human tumor cell lines. Cancer Chemother Pharmacol 1994;33:331–339.
[31] Liebmann J, Cook J, Mitchell J, et al. Solvent for paclitaxel, and toxicity. Lancet 1993;342:1428.
[32] Ho EA, Soo PL, Allen C, et al. Impact of intraperitoneal, sustained delivery of paclitaxel on the expression of P-glycoprotein in ovarian tumors. J Control Release 2007;117:20–27.
[33] Singla AK, Garg A, Aggarwal D. . Paclitaxel and its formulations. Int J Pharm 2002;235:179–192.
[34] Baek J-S, Cho C-W. . Controlled release and reversal of multidrug resistance by co-encapsulation of paclitaxel and verapamil in solid lipid nanoparticles. Int J Pharm 2015;478:617–624.
[35] Patil Y, Sadhukha T, Ma L, et al. Nanoparticle-mediated simultaneous and targeted delivery of paclitaxel and tariquidar overcomes tumor drug resistance. J Control Release 2009;136:21–29.
[36] Sarisozen C, Vural I, Levchenko T, et al. PEG-PE-based micelles co-loaded with paclitaxel and cyclosporine A or loaded with paclitaxel and targeted by anticancer antibody overcome drug resistance in cancer cells. Drug Deliv 2012;19:169–176.